

Fitting DVCS at NLO and beyond

K. Kumerički¹, D. Müller², K. Passek-Kumerički^{3†}

¹Department of Physics, Faculty of Science, University of Zagreb, Croatia

²Institut für Theoretische Physik II, Ruhr-Universität Bochum, Germany

³Theoretical Physics Division, Rudjer Bošković Institute, Croatia

Abstract

We outline the twist-two analysis of deeply virtual Compton scattering (DVCS) within the conformal partial wave expansion of the amplitude, represented as a Mellin–Barnes integral. The complete next-to-leading order results, including evolution, are obtained in the $\overline{\text{MS}}$ and a conformal factorization scheme. Within the latter, exploiting conformal symmetry, the radiative corrections are evaluated up to next-to-next-to-leading order. Using a new proposed parameterization for GPDs, we study the convergence of perturbation theory and demonstrate for H1 and ZEUS measurements that our formalism is suitable for a fitting procedure of DVCS observables. We comment on a recent claim of a breakdown of collinear factorization and show that a Regge-inspired Q^2 scaling law is ruled out by small x_{Bj} DVCS data.

1 Introduction

The proton structure has been widely explored in inclusive measurements, mainly in deeply inelastic lepton-proton scattering (DIS). Here the scattering essentially occurs due to the exchange of a virtual boson (photon) between lepton and a single parton, and so one can access *parton distribution functions* (PDFs). These universal, however, convention-dependent functions $q_a(x)$ are interpreted as probabilities that partons of certain flavour a will be found with given longitudinal momentum fraction x . Since the PDFs are naturally defined in a translation invariant manner, they do not carry information about the transversal distribution of partons. Some information about transversal degrees of freedom can be obtained from elastic lepton-proton scattering. Namely, the electromagnetic form factors $F_{1,2}(t)$ are Fourier transforms of the electric and magnetic charge distribution in nucleon, and can be, e.g., in the infinite momentum frame, interpreted as probability that partons are found at some transversal distance \mathbf{b} from the center-of-mass. However, one should not assume that a realistic probability distribution of partons, given by a two-variable function $q(x, \mathbf{b})$ is simply a direct product, i.e., $q(x) \otimes q(\mathbf{b})$, of two probability functions. Rather it is anticipated that longitudinal and transversal degrees of freedom have a cross talk, e.g., as x gets bigger partons carry more of the nucleon longitudinal momentum and are expected to be closer to the proton center, and thus the \mathbf{b} dependence in $q(x, \mathbf{b})$ should become narrower with increasing x .

[†]Based on talks presented by the authors at *Elastic and Diffractive Scattering 2007*, DESY Hamburg, Germany; *Exclusive Reactions at High Momentum Transfer*, JLab Newport News, US; *The 6th Circum-Pan-Pacific Symposium on High Energy Spin Physics*, UBC Vancouver, Canada; *XII Workshop on High Energy Spin Physics*, JINR Dubna, Russia; and *New Trends in High-Energy PHYSICS*, Yalta, Ukraine.

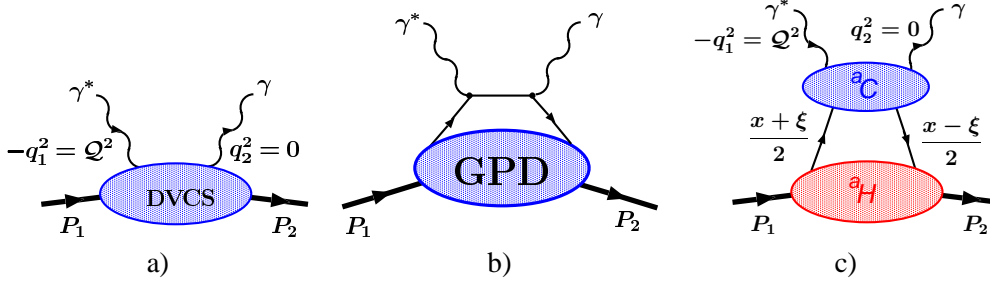


Fig. 1: a) DVCS. b) Leading-order perturbative contribution to DVCS. c) Factorization (to all orders in α_s) on an example of special parity-even, helicity conserving contribution $^a\mathcal{H}$, Eq. (10).

The three dimensional distribution of partons in the nucleon can be addressed within more general objects, called *generalized parton distributions* (GPDs) [1–3]. Such distributions can be revealed by analyzing hard exclusive leptonproduction of mesons or photon. The theoretical description of the former processes is perhaps more problematic, but they offer a direct view into individual flavour GPDs. To the latter one the *deeply virtual Compton scattering* (DVCS) process contributes, where one photon has a large virtuality. DVCS is theoretically considered as the cleanest probe of GPDs, however, here only certain flavour combinations of GPDs appear.

The non-forward Compton scattering process is described by the Compton tensor

$$T_{\mu\nu}(q, P, \Delta) = \frac{i}{e^2} \int d^4x e^{ix \cdot q} \langle P_2, S_2 | T j_\mu(x/2) j_\nu(-x/2) | P_1, S_1 \rangle, \quad (1)$$

where $q = (q_1 + q_2)/2$, $P = P_1 + P_2$ and $\Delta = P_2 - P_1$. The generalized Bjorken limit corresponds to $Q^2 = -q^2 \rightarrow \infty$ with the scaling variables

$$\xi = \frac{Q^2}{P \cdot q}, \quad \eta = -\frac{\Delta \cdot q}{P \cdot q}, \quad (2)$$

and the momentum transfer squared Δ^2 being fixed. Note that in the forward case, i.e., $\Delta \rightarrow 0$, the hadronic DIS tensor $W_{\mu\nu}$ is related to the *forward* Compton scattering tensor by the optical theorem

$$W_{\mu\nu} = \Im T_{\mu\nu}(q, P = 2p, \Delta = 0)/(2\pi), \quad (3)$$

where $p = P_1 = P_2$ and $\xi \rightarrow x_{Bj}$.

In DVCS – Fig. 1a – the virtuality of the incoming photon $Q^2 = -q_1^2$ is large while the final photon is on-shell. The skewness parameter η and the Bjorken-like scaling parameter ξ are then equal to twist-two accuracy, i.e., $\eta = \xi + \mathcal{O}(1/Q^2)$. In the generalized Bjorken limit, similarly as for DIS structure functions, the amplitude factorizes [4] into long- and short-distance contributions (Fig.1b and c): short-distance physics is perturbatively calculable Compton scattering on a parton, while long-distance physics is encoded in a non-perturbative amplitude for a parton being emitted and later reabsorbed by the nucleon. The latter *amplitude* is called GPD. The factorization of long- and short-distance contributions is based on the reshuffling of divergent contributions from the perturbative calculable hard-scattering part to the universal, i.e., process

independent GPDs. Although GPDs are universal they depend on the scheme convention and also on the order of the approximation to which one is able to perform the perturbative calculation.

The GPDs with even parity, considered here, are defined as

$$^qF(x, \eta, \Delta^2) = \int \frac{dz^-}{2\pi} e^{ixP^+z^-} \langle P_2 | \bar{q}(-z) \gamma^+ q(z) | P_1 \rangle \Big|_{z^+=0, \mathbf{z}_\perp=\mathbf{0}}, \quad (4)$$

$$^GF(x, \eta, \Delta^2) = \frac{4}{P^+} \int \frac{dz^-}{2\pi} e^{ixP^+z^-} \langle P_2 | G_a^{+\mu}(-z) G_{a\mu}^+(z) | P_1 \rangle \Big|_{z^+=0, \mathbf{z}_\perp=\mathbf{0}}, \quad (5)$$

and similarly for odd parity. Furthermore, it is convenient to make a decomposition,

$$^aF = \frac{\bar{u}(P_2) \gamma^+ u(P_1)}{P^+} ^aH + \frac{\bar{u}(P_2) i \sigma^{+\nu} u(P_1) \Delta_\nu}{2MP^+} ^aE, \quad a = q, G, \quad (6)$$

into helicity conserving and non-conserving generalized form factors. The Compton tensor (1) is analogously decomposed into Compton form factors with corresponding parity and helicity properties. In the forward limit ($\Delta \rightarrow 0$) GPDs reduce to PDFs. Together with sum rules, e.g., relating GPDs to electromagnetic form factors, this provides constraints that are important for GPD modelling. But as they do not constrain much the skewness (η) dependence, modelling is still a difficult problem. One guiding feature is a polynomiality property of GPDs: n -th (Mellin) moment of GPD is even polynomial in η of order n or $n \pm 1$. Similar polynomiality will be obeyed also by conformal moments which are just linear combination of Mellin moments. The usefulness of the GPDs has also been widely realized in connection with the spin problem, since they encode the angular momentum carried by the individual parton species, as explicated by the Ji's sum rule [3]. For recent detailed account of GPDs and their properties, we refer to [5].

In the following we first briefly comment on the work in Ref. [6], which claims that collinear factorization breaks down. We then proceed with the outline of the perturbative QCD approach to DVCS that is based on the conformal partial wave expansion, represented as Mellin-Barnes integral and described in detail in Refs. [7, 8]. Here, as in Refs. [8–10], we concentrate on the dominant Compton form factor \mathcal{H} corresponding to parity-even helicity-conserving GPD H . For simplicity, we present only the results for the singlet part which is dominant for the kinematics of collider experiments. We shortly discuss our phenomenological analysis of H1 and ZEUS DVCS data. Finally, we conclude.

2 Does collinear factorization break down?

Here we would like to comment on a recent claim of an observed breakdown of collinear factorization [6], which the authors consider as a general feature of deeply exclusive leptonproduction. This claim originated from a divergent result that was found by convoluting a model GPD with the hard-scattering part in the handbag approximation, cf. Fig. 1b. In our opinion the GPD model employed by Ref. [6] suffers from ultraviolet and/or infrared divergencies. A matching procedure with the collinear factorization approach is impossible, since the model does not respect the ultraviolet behavior of QCD.

- Divergences in a non-perturbative model that can not be cured within the factorization approach have to be removed by hand, e.g., by an effective cut off, before the model can

be utilized. Convoluting a model GPD, even a finite one, with the hard-scattering part, and obtaining undefined result does not in itself constitute a proof of a breakdown of collinear factorization.

We recall that the collinear factorization approach has been worked out for deeply exclusive leptonproduction to NLO [11, 12], including evolution, and its quantitative features have been extensively studied. Below we report about our own investigations of DVCS beyond this order.

We find it interesting that the analysis of Ref. [6] resulted in an infinite DVCS amplitude. Since it was claimed that this is a necessary consequence of Regge behavior, we would like to offer our opinion about the origin of these divergences. Let us remind that the field-theoretical definition (4) of GPDs states that they are generalized functions in the mathematical sense rather than regular ones [1]. To shorten the discussion and without loss of generality, we will employ this fact for the evaluation of the convolution integral [13].

The non-perturbative dynamics of the GPD utilized in Ref. [6] is described by a parton model. It is supposed that the collective spectator has leading Regge behavior, i.e., $0 < \alpha < 1$, and interacts *point-likely* with the active *spin-zero* constituents. This reduction of the spin content induces a factor x which is taken outside of the GPD and leads to a *non-standard* representation [14]. This causes a mathematical paradox for “good” GPDs. Namely, the inverse, i.e., $1/x$, moment of a GPD is defined, contrarily to what one expects on general grounds, while in the forward limit the inverse moment of the resulting PDF is divergent for $0 < \alpha < 1$. Obviously, to be consistent, a *non-standard* GPD must contain some “bad” terms. The solutions are (i.) to reject such a GPD model, (ii.) to put the “bad” part in the central region $-\eta \leq x \leq \eta$, where it serves as a counterterm, and (iii.) to define the inverse moment for the PDF. Our choice in Eq. (7) below corresponds to the last possibility and the illustration of thus obtained “good” GPDs. Furthermore, we stress that the *point-like* coupling of the constituents ties the high-energy and the ultraviolet behavior. The treatment of divergencies¹ as part of modelling was not specified in Ref. [6] and, consequently, the resulting GPDs contain ambiguous terms.

- We consider the GPD model [6] in its presented form as mathematically ill-defined.

An elegant method to overcome all these obstacles is to consider the GPD model [6] as an analytic function of the parameter α . This allows removal of ultraviolet (or infrared) divergencies, except at discrete values of α , e.g., $\alpha = 0$ and $\alpha = 1$. Possible version of the GPD model part that originates from the leading Regge behavior reads in the region $-\eta \leq x \leq 1$ as follows

$$H(x, \eta) = -\frac{N}{2\alpha} \frac{x}{\eta} \left[\theta(x + \eta) \left(\frac{x + \eta}{1 + \eta} \right)^{-\alpha} - \theta(x - \eta) \left(\frac{x - \eta}{1 - \eta} \right)^{-\alpha} \right]. \quad (7)$$

Up to terms which live only in the central region $-\eta \leq x \leq \eta$, and Regge non-leading terms, this expression coincides with the result given in Ref. [6]. Note that we consider $(\dots)^{-\alpha}$ as generalized functions, which might be expressed using conventional “+” definitions and some additional subtraction terms. The forward limit yields the PDF $H(x, \eta = 0) = Nx^{-\alpha}(1 - x)$

¹In the model one can choose to have ultraviolet, infrared, or both kinds of divergencies, however, one can not get rid of all of them. After momentum integration the GPDs will always suffer from the same illness, which is not primarily related to the high-energy behavior, rather, it is the generic feature of the underlying simplifications.

and its inverse moment, i.e., $\int_0^1 dx x^{-1-\alpha}(1-x) = 1/\alpha(\alpha-1)$, is defined. Armed with a clear mathematical language [13], we calculate the convolution with the hard scattering part and get a finite result, however, with an ‘unusual’ negative overall sign:

$$\mathcal{H}(\xi) = \int_{-1}^1 dx \frac{2x}{\xi^2 - x^2 - i\epsilon} H(x, \xi) = -\frac{N\pi}{2\alpha} (2\xi)^{-\alpha} \left[i - \cot\left(\frac{\pi\alpha}{2}\right) + O(\xi) \right] + O(\xi^0). \quad (8)$$

- The reported divergences in Ref. [6] do *not* show up in the leading Regge behavior. They arise from ill-defined subtractions, entirely related to non-leading Regge behavior.

Our inspection revealed that the ambiguous part in the GPD model [6], affected by ultraviolet and/or infrared divergences, possesses non-leading Regge behavior. It shows up only in the central GPD region and causes the observed divergences in the DVCS amplitude.

The fact that the GPD representation is not unique was pointed out in Refs. [14, 15]. We recall that numerous QCD model evaluations confirm within the *standard* GPD definition a finite and continuous behavior at the cross-over points $x = \pm\eta$, see Refs. [5, 16] and references therein. In contrast to the representation used in Ref. [6], Regge behavior of standard GPDs is continuous at the cross-over points, e.g., for $\alpha < 1$:

$$\begin{array}{cc} \frac{x}{\eta} \left[\left(\frac{x-\eta}{1-\eta} \right)^{-\alpha} - \left(\frac{x+\eta}{1+\eta} \right)^{-\alpha} \right], & \frac{1}{\eta} \left[\left(\frac{x+\eta}{1+\eta} \right)^{1-\alpha} - \left(\frac{x-\eta}{1-\eta} \right)^{1-\alpha} \right] \text{ for } x \rightarrow \eta, \quad \eta \leq x. \\ \text{spin-0 partons} & \text{spin-1/2 partons} \end{array} \quad (9)$$

If one chooses the standard GPD representation, the s -channel view in Ref. [6] confirms the implementation of Regge behavior in common GPD models [16] and our approach. To see this, one simply convolutes the spectral function (9) of Ref. [6] and the models (19) and (21) of Ref. [17] with respect to the spectator mass λ . Doing so one finds the r.h.s. in (9).

Finally, in Ref. [6] it was suggested to utilize so-called Regge-exchange amplitudes for phenomenology. These amplitudes are not universal and possess a typical $s^{\alpha(t)} \sim (Q^2/\xi)^{\alpha(t)}$ Regge behavior, which yields a softening of Bjorken scaling. Let us recall that Regge phenomenology has been developed out of S -matrix theory, i.e., for processes with asymptotic states, e.g., $q_1^2 = q_2^2 = 0$, in lack of a dynamical understanding of strong interaction phenomena. Hence, one might surmise that the implementation of Regge-behavior in a parton model within virtual constituents and *point-like* interaction may predict unrealistic scaling for off-shell amplitudes. A last objection arises when the claimed scaling behavior [6] is confronted with DVCS data in the high-energy region (see Sect. 5 below):

- The generic $(Q^2/\xi)^{\alpha(t)}$ behavior of Regge-exchange amplitudes is ruled out by experiment.

We emphasize that this statement is based on experimental data, presently available. Our investigation, given below, will show where perturbation theory reveals itself and in which kinematics the high-energy limit spoils the Bjorken limit. It turns out that this is rather a universal feature, which is tied to the ultraviolet behavior in QCD.

3 Deeply virtual Compton scattering

Besides DVCS, the Bethe-Heitler (BH) brehmstrahlung process contributes to the measured hard photon leptonproduction off a proton. The BH amplitude, known in leading order of the QED fine structure constant, is expressed in terms of the known electromagnetic form-factors. Generally, there are two types of DVCS experiments: collider experiments and fixed target experiments. The former usually provide information in the phase space $10^{-4} \lesssim \xi \lesssim 10^{-1}$ and $1 \text{ GeV}^2 \lesssim Q^2 \lesssim 100 \text{ GeV}^2$, and such are H1 and ZEUS experiments at HERA. The main observables here are total and differential DVCS cross sections, however, also the measurement of beam charge asymmetry is feasible. For the fixed target experiments, such as Hall A, Hall B (CLAS) at JLAB, and HERMES at DESY, the DVCS–BH interference term can be more easily accessed via single beam, target spin and beam charge (HERMES) asymmetries, while the investigated phase space covers the so-called valence quark region, i.e., $0.05 \lesssim \xi \lesssim 0.3$ within $1 \text{ GeV}^2 \lesssim Q^2 \lesssim 10 \text{ GeV}^2$.

One can express \mathcal{H} as a convolution (Fig.1c) over the longitudinal momentum fraction x

$$^a\mathcal{H}(\xi, \Delta^2, Q^2) = \int dx \, ^aC(x, \xi, Q^2/\mu^2) \, ^aH(x, \eta = \xi, \Delta^2, \mu^2), \quad (10)$$

where μ^2 is a factorization scale that separates short- and long-distance dynamics and is often taken as $\mu^2 = Q^2$. Here the index $a \in \{\text{NS}, \text{S}(\Sigma, G)\}$ denotes either non-singlet or singlet parts, where to latter both quarks (Σ) and gluons (G) contribute.

The coefficient functions C^a are perturbative quantities which describe $q\gamma^* \rightarrow q\gamma$ and $g\gamma^* \rightarrow g\gamma$ subprocesses. The well known leading-order (LO) contribution to C^a is actually a pure QED process (Fig. 1b). The next-to-leading order (NLO) contribution — the first order in α_s — has been calculated by various groups [11]. Obviously, to stabilize the perturbation series and investigate its convergence one needs the second order in α_s , i.e., next-to-next-to-leading order (NNLO) contributions. The importance of NNLO in singlet case is amplified by the fact that at LO photons scatter only off charged partons, whereas gluons start contributing at NLO.

The GPDs aH are intrinsically non-perturbative quantities whose form at some initial scale Q_0 has to be deduced by some non-perturbative methods (lattice calculation, fit to data, etc.). The evolution to the factorization scale of interest is governed by perturbation theory, cf. [8, 10] for LO examples. The anomalous dimensions of non-diagonal operators were calculated up to NLO [18]. Still, evolution at NLO is numerically not easy to implement, and has been investigated beyond NLO only recently, using the procedure explained below [8].

Instead of using the convolution (10) one can equivalently use the sum over the conformal moments, and the singlet contribution then takes the form

$$^S\mathcal{H}(\xi, \Delta^2, Q^2) = 2 \sum_{j=0}^{\infty} \xi^{-j-1} C_j(Q^2/\mu^2, \alpha_s(\mu)) \, H_j(\eta = \xi, \Delta^2, \mu^2), \quad (11)$$

where $C_j = ({}^\Sigma C_j, {}^G C_j)$ and $H_j = ({}^\Sigma H_j, {}^G H_j)$ are conformal moments. They are analogous to common Mellin moments used in DIS but the integral kernel x^j is replaced by Gegenbauer polynomials $C_j^{3/2}(x)$ and $C_j^{5/2}(x)$, which are solutions of LO evolution equations for quarks and gluons, respectively. Unfortunately, the series (11) only converges in the unphysical region.

Hence, it is necessary to resum this series, e.g., by means of the Mellin-Barnes integral [8]

$$\mathcal{H}(\xi, \Delta^2, Q^2) = \frac{1}{2i} \int_{c-i\infty}^{c+i\infty} dj \xi^{-j-1} \left[i + \tan\left(\frac{\pi j}{2}\right) \right] C_j(Q^2/\mu^2, \alpha_s(\mu)) \mathbf{H}_j(\xi, \Delta^2, \mu^2). \quad (12)$$

The advantages of using conformal moments, i.e., Mellin-Barnes representation, are manifold: it enables a simple inclusion of evolution, it allows for an efficient and stable numerical treatment, and it opens a new approach to modelling of GPDs. Finally, by making use of conformal operator product expansion (OPE) and known NNLO DIS results, it enables the assessment of NNLO contributions, to which we now turn.

4 Conformal approach to DVCS beyond NLO

Neither Wilson coefficients nor anomalous dimensions are calculated in non-forward kinematics at NNLO (only so-called quark bubble insertions were partly evaluated [19]). To access the NNLO of non-forward Compton scattering, we use the conformal approach, making it possible to calculate relevant objects using only diagonal results of forward Compton scattering, i.e., DIS.

DVCS belongs to a class of two-photon processes (DIS, DVCS, two-photon production of hadronic states ...) calculable by means of the OPE, $T_{\mu\nu}(q, P, \Delta) \rightarrow C_j O_j$, for which the use of generalized Bjorken kinematics and conformal symmetry enables a unified description. While massless QCD is conformally invariant at tree level, this invariance is broken at the loop level since renormalization introduces a mass scale, leading to the running of the coupling constant ($\beta \neq 0$). Assuming the existence of a non-trivial fixed point α_s^* , i.e., $\beta(\alpha_s^*) = 0$, the conformal OPE (COPE) prediction for Wilson coefficients in general kinematics reads [20]

$$C_j(\alpha_s^*) = c_j(\alpha_s^*) {}_2F_1\left(\frac{(2+2j+\gamma_j(\alpha_s^*))/4, (4+2j+\gamma_j(\alpha_s^*))/4}{(5+2j+\gamma_j(\alpha_s^*))/2} \middle| \frac{\eta^2}{\xi^2}\right) \left(\frac{\mu^2}{Q^2}\right)^{\gamma_j(\alpha_s^*)/2}. \quad (13)$$

For $\eta = 0$ equation (13) reduces to the DIS Wilson coefficients $C_j \rightarrow c_j$ and thus fixes the normalization c_j . The choice $\eta = \xi$ corresponds to DVCS in the conformal limit. The anomalous dimensions governing the evolution are diagonal and the same as in DIS.

For a general factorization scheme, e.g., the $\overline{\text{MS}}$ scheme, the conformal symmetry breaking occurs also due to the renormalization of the composite operators and causes the appearance of non-diagonal anomalous dimensions $\gamma_{jk} = \delta_{jk}\gamma_j + \gamma_{jk}^{\text{ND}}$. This induces a mixing of both operators, i.e., GPDs, and Wilson coefficients under evolution. In the kinematical forward limit ($\eta = 0$) the diagonal evolution equations are again obtained, i.e., the DIS case corresponds to the COPE result. For DVCS, evaluated in the $\overline{\text{MS}}$ scheme, there appear also conformal symmetry breaking terms which are not proportional to β , i.e., the non-diagonal terms survive.

The non-diagonal terms of anomalous dimensions encountered in $\overline{\text{MS}}$ scheme can be removed by a finite renormalization [20], i.e., by a specific choice of the factorization scheme

$$C^{\overline{\text{MS}}} O^{\overline{\text{MS}}} = C^{\overline{\text{MS}}} B B^{-1} O^{\overline{\text{MS}}} = C^{\overline{\text{CS}}} O^{\overline{\text{CS}}}. \quad (14)$$

In this new scheme, called conformal subtraction ($\overline{\text{CS}}$) scheme, all non-diagonal terms are "pushed" to the β proportional part $\gamma_{jk}^{\overline{\text{CS}}} = \delta_{jk}\gamma_k + \beta/g\Delta_{jk}$. Furthermore, since there is an ambiguity in

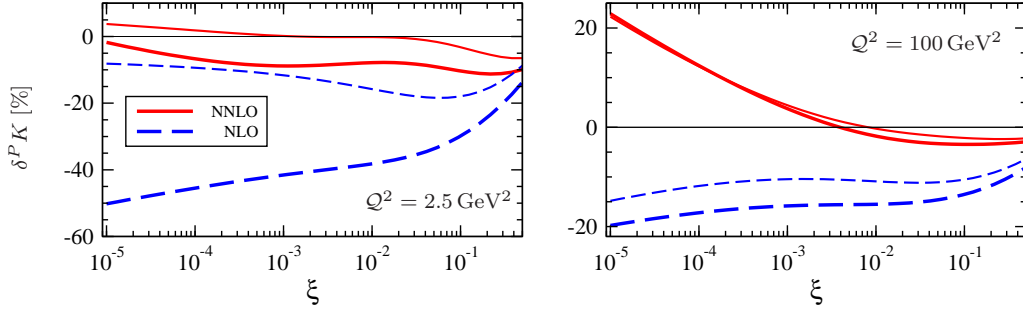


Fig. 2: Relative NLO and NNLO corrections (19) in the $\overline{\text{CS}}$ scheme ($\Delta^2 = 0.25\text{GeV}^2$, input scale $Q_0^2 = 2.5\text{GeV}^2$). Thick [thin] lines denote “hard” [“soft”] gluon scenarios: $N_G = 0.4$, $\alpha_G(0) = \alpha_\Sigma(0) + 0.05$ [$N_G = 0.3$, $\alpha_G(0) = \alpha_\Sigma(0) - 0.02$].

$\overline{\text{MS}} \rightarrow \overline{\text{CS}}$ rotation matrix, by judicious choice δB one can “push” mixing under evolution to NNLO. Hence, in $\overline{\text{CS}}$ scheme, which we are using, the unknown correction Δ_{jk} starts at NNLO and it can be additionally suppressed by the choice of an appropriate initial condition. Finally, we express our result in $\overline{\text{CS}}$ scheme as

$$C_j^{\overline{\text{CS}}} = \sum_{k=j}^{\infty} C_k(\alpha_s(Q)) \mathcal{P} \exp \left\{ \int_Q^\mu \frac{d\mu'}{\mu'} \left[\gamma_j(\alpha_s(\mu')) \delta_{kj} + \frac{\beta}{g} \Delta_{kj}(\alpha_s(\mu')) \right] \right\}, \quad (15)$$

with $C_k(\alpha_s(Q))$ obtained from the $\eta = \xi$ limit of Eq. (13) and using $c_j(\alpha_s)$. As stated above the Δ_{kj} mixing term appears at NNLO and is neglected. We take c_j and γ_j calculated to NNLO order from Refs. [21], and obtain the DVCS prediction to NNLO in the $\overline{\text{CS}}$ scheme.

5 Results

We have used the formalism described in the preceding sections to investigate the size of NNLO corrections to non-singlet [9] and singlet Compton form factors [10], to obtain complete (non-diagonal evolution included) $\overline{\text{MS}}$ NLO predictions [8], and to perform fits, in both $\overline{\text{MS}}$ and $\overline{\text{CS}}$ schemes, to DVCS and DIS data and to extract information about GPDs [8].

One can use a simple Regge-inspired ansatz for GPDs at the input scale

$$\mathbf{H}_j(\eta, \Delta^2, Q_0^2) = \begin{pmatrix} N'_\Sigma F_\Sigma(\Delta^2) B(1+j-\alpha_\Sigma(0), 8) \\ N'_G F_G(\Delta^2) B(1+j-\alpha_G(0), 6) \end{pmatrix} + \mathcal{O}(\eta^2), \quad (16)$$

with (p_a is a flavour dependent integer)

$$\alpha_a(\Delta^2) = \alpha_a(0) + 0.15\Delta^2, \quad F_a(\Delta^2) = \frac{j+1-\alpha_a(0)}{j+1-\alpha_a(\Delta^2)} \left(1 - \frac{\Delta^2}{M_0^{a2} + jM_\Delta^{a2}} \right)^{-p_a}. \quad (17)$$

Here α_a are effective Regge-trajectories and F_a at $j = 0$ are partonic form factors, which are modelled as product of a monopole factor, arising from the effective Regge exchange, and an

impact form factor. The Δ^2 -dependence of higher moments could be easily pinned down from realistic lattice measurements, see Ref. [22] and references therein for the present status of simulations in the flavour sector. The ansatz is based on modelling the t -channel contributions of the GPDs in terms of SO(3) partial waves [23] at a low input scale and then using analyticity, implicitly tied to Lorentz symmetry (polynomiality of GPD moments), to extend the GPD support [7]. Our assumption is that at a rather low input scale, i.e., photon virtuality, Regge behavior is present in the GPD moments and can be effectively modelled by poles in the complex conformal spin plane. Doing that in such a way yields GPDs that behave continuously at the cross-over point and can so be smoothly incorporated in the factorization approach. We emphasize that this is compatible with the s -channel view [6], if it would be presented in an appropriate representation, cf. Eq. (9). In the forward case ($\Delta = 0$) ansatz (16) is equivalent to the standard building blocks for PDFs:

$$\Sigma(x) = N'_\Sigma x^{-\alpha_\Sigma(0)} (1-x)^7, \quad G(x) = N'_G x^{-\alpha_G(0)} (1-x)^5. \quad (18)$$

We relied in our ansatz (16) only on the leading SO(3) partial wave, which can be for $\eta \lesssim 0.3$ safely approximated by a constant. The work on a more flexible η -dependent ansatz, i.e., the model dependent resummation of SO(3) partial waves is in progress.

We have performed the analysis of radiative corrections with generic parameters and made fits of relevant parameters N_Σ , $\alpha_\Sigma(0)$, M_0^Σ , N_G , $\alpha_G(0)$, M_0^G (since of $j \sim 0$ dominance M_Δ^a can be safely set to zero). We introduce now the quantities that we utilize as a measures of the scheme dependence and, foremostly, as indicators for the convergence of the perturbation series. It is natural to employ for this purpose the ratios of Compton form factors, i.e., the corresponding modulus and phase difference, at order $N^P\text{LO}$ to those at order $N^{P-1}\text{LO}$, where $P = \{0, 1, 2\}$ stands for LO, NLO, and NNLO order, respectively:

$$\delta^P K = \frac{|\mathcal{H}^{N^P\text{LO}}|}{|\mathcal{H}^{N^{P-1}\text{LO}}|} - 1, \quad \delta^P \varphi = \arg \left(\frac{\mathcal{H}^{N^P\text{LO}}}{\mathcal{H}^{N^{P-1}\text{LO}}} \right). \quad (19)$$

The phase differences are small, and we will not comment on them here further. The NLO corrections to the moduli in $\overline{\text{MS}}$ and $\overline{\text{CS}}$ schemes have a similar ξ -shape, where $\overline{\text{MS}}$ corrections are generally larger. The relative NLO and NNLO corrections in $\overline{\text{CS}}$ scheme are depicted in Fig. 2. From the left panel, showing corrections at the input scale, we realize that the large negative NLO corrections to the modulus in the ‘hard’ gluon scenario (thick dashed) are shrunk at NNLO to less than 10% (thick solid), in particular in the small ξ region. In the ‘soft’ gluon case the NNLO corrections (thin solid) are $\pm 5\%$. For $\xi \sim 0.5$, the corrections are reduced only unessentially and are around 5% and 10% at both NLO and NNLO level. If evolution is switched on (right panel), our findings drastically change. For $5 \cdot 10^{-2} \lesssim \xi$ NNLO corrections are stabilized on the level of about 3% at $Q^2 = 100 \text{ GeV}^2$. But they start to grow with decreasing ξ and reach at $\xi \approx 10^{-5}$ the 20% level. As in DIS, this breakdown of perturbation theory at small ξ in DVCS obviously stems from evolution and is thus universal, i.e., process independent. The large change of the scaling prediction within the considered order does not influence the quality of fits, and, in particular, the possibility of relating DVCS and DIS data. Hence, the problem of treatment or resummation of these large corrections is relevant primarily to our partonic interpretation of the nucleon content.

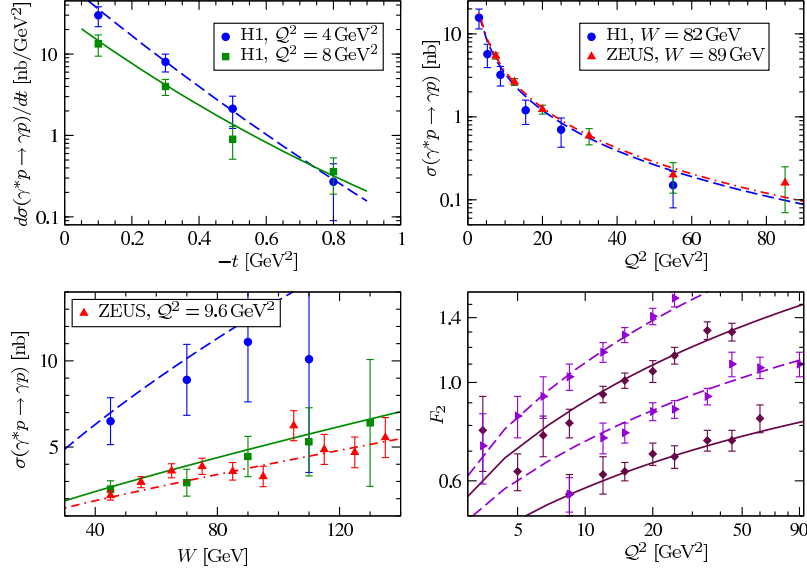


Fig. 3: Simultaneous fit to the DVCS and DIS data in the $\overline{\text{CS}}$ scheme to NNLO. Upper left panel DVCS cross section for $Q^2 = 4 \text{ GeV}^2$ and $W = 71 \text{ GeV}$ (circles, dashed) as well as $Q^2 = 8 \text{ GeV}^2$ and $W = 82 \text{ GeV}$ (squares, solid) [27]. Upper right panel DVCS cross section ($|\Delta^2| < 1 \text{ GeV}^2$) versus Q^2 for $W = 82 \text{ GeV}$ (H1, circles, dashed) and $W = 89 \text{ GeV}$ (ZEUS, triangles, dash-dotted) [28]. Lower left panel DVCS cross section versus W $Q^2 = 4 \text{ GeV}^2$ (H1, circles, dashed), $Q^2 = 8 \text{ GeV}^2$ (H1, squares, solid), and $Q^2 = 9.6 \text{ GeV}^2$ (ZEUS, triangles, dash-dotted). Lower right panel shows $F_2(x_{\text{Bj}}, Q^2)$ versus Q^2 for $x_{\text{Bj}} = \{8 \cdot 10^{-3}, 3.2 \cdot 10^{-3}, 1.3 \cdot 10^{-3}, 5 \cdot 10^{-4}\}$ [29].

As long as we precisely define the treatment of the evolution operator, perturbative QCD can be employed as a tool for analyzing data also in the small ξ region. However, it might be expected that in meson leptonproduction dominant perturbative corrections [12, 24] at small ξ in the hard scattering amplitude are not connected only to the evolution and should be resummed [25].

The Mellin-Barnes integral approach offers the possibility for a fast and numerically stable analysis. Our numerical routine is designed for the purpose of fitting DVCS (and DIS) observables and testing various GPD ansätze. A fit example for measurements of the H1 and ZEUS collaborations [26–29] is presented in Fig. 3 at NNLO. In these collider experiments the DVCS cross section can be accessed and is given, up to ξ and $\langle -\Delta^2 \rangle / 4M^2 \sim 0.05$ proportional corrections, at leading twist as

$$\frac{d\sigma}{d\Delta^2}(W, \Delta^2, Q^2) \approx \frac{4\pi\alpha^2}{Q^4} \xi^2 |\mathcal{H}|^2 \left(\xi = \frac{Q^2}{2W^2 + Q^2}, \Delta^2, Q^2 \right). \quad (20)$$

For fixed ξ we have the canonically expected scaling behavior $1/Q^4$, which is strongly modified by the resummation of $\log Q^2$ terms.

As one can realize from Fig. 3 the quality of a simultaneous DVCS and DIS fit within our ansatz (16) is quite good, namely, $\chi^2/\text{d.o.f.} = 0.77$. We only observed bad fits to LO accuracy, which originate from the fact that the normalization of the DVCS amplitude for fixed Δ^2 is not adjustable, since we took only the leading $\text{SO}(3)$ partial wave. We already demonstrated that taking the next-to-leading $\text{SO}(3)$ partial wave leads to good LO fits [30]. Note that this is nothing

else but a minimal version of the so-called dual GPD parameterization [23], used in Ref. [31]. Let us emphasize that our fits support the following functional form of CFFs in the small ξ -region:

$$|\mathcal{H}(\xi, \Delta^2, Q^2)| \sim N(\xi, Q^2, \Delta^2) \left(\frac{\xi_0}{\xi} \right)^{\alpha^{\text{eff}}(\Delta^2, Q^2)}, \quad (21)$$

where $N(\xi, Q^2, t)$ and $\alpha^{\text{eff}}(t, Q^2)$ effectively describe the change of the normalization and slope due to the predicted scaling violations, i.e., mainly arising from evolution.

In contrast, the so-called Regge-exchange amplitude [6] yields a behavior which is rather similar to the Regge behavior of on-shell amplitudes ($W^2 \equiv s$)

$$|\mathcal{H}(\xi, \Delta^2, Q^2)| \sim N'(\xi, \Delta^2) \left(\frac{W^2}{W_0^2} \right)^{\alpha(\Delta^2)}. \quad (22)$$

Here the normalization factor $N'(\xi, \Delta^2)$ can for internal consistency of the model [6] only weakly depend on $\xi \sim Q^2/2W^2$ and so it can be safely neglected in the small ξ kinematics. This prediction has so far been compared only with exclusive leptonproduction data [32–34] in the valence quark region [6], which is not conclusive ². As spelled out above, the DVCS amplitude can be described to LO accuracy, where gluons are absent in the hard scattering part. Hence, for the sake of illustration we consider it legitimate to confront the Regge-exchange amplitude [6] within a pomeron Regge trajectory $\alpha(\Delta^2) = 1 + 0.25\Delta^2 < 1$ with high-energy DVCS data. As one can immediately realize from Eqs. (20) and (22) for fixed W the cross section should not scale with Q^2 , which is in conflict with the observation, describable by a $(Q^2)^{-1.54 \pm 0.09 \pm 0.04}$ fit [27], as shown in the upper right panel in Fig. (3). Confronting Eq. (22) with the few experimental data points for fixed ξ [27] also disfavors the claimed Regge scaling. We note that a BFKL evaluation of the DVCS amplitude indicates a rather intricate ξ and Q^2/Δ^2 dependencies in the high-energy limit [35], which seems not to support the conjectured Regge behavior [6], borrowed from on-shell amplitudes.

Turning now to presentation of the GPDs resulting from the fits, we recall that Fourier transform of GPDs for $\eta = 0$,

$$H(x, \mathbf{b}) = \int \frac{d^2 \Delta}{(2\pi)^2} e^{-i\mathbf{b} \cdot \Delta} H(x, \eta = 0, \Delta^2 = -\Delta^2), \quad (23)$$

can be interpreted in the infinite momentum frame as probability density [36], see Fig. 4b. The average transversal parton distance squared $\langle \mathbf{b}^2 \rangle$ is given by the GPD slope $B = \langle \mathbf{b}^2 \rangle/4$, shown in Fig. 4a. Although gluons are perturbatively suppressed in DVCS, one has a handle on them via the Q^2 evolution. The found value for $\langle \mathbf{b}^2 \rangle$ is compatible with the analysis for deeply exclusive photo and leptonproduction of J/ψ [37]. The results confirm the picture, mentioned in the

²Note that from present fixed target data it is rather difficult to judge on any predicted Q^2 scaling behavior, since kinematical variables are strongly correlated for a large Q^2 lever arm and, moreover, to access the twist-two sector in exclusive meson leptonproduction one has to extract the cross section that arises from the exchange of a longitudinal polarized photon. Within small Q^2 lever arm and small t , DVCS [33] indicates a canonical scaling which might be logarithmical modified [8], and is also still consistent with Regge scaling within a rather low $\alpha(\ll t \gg) = 0.15$ parameter [5]; as in DIS, exact canonical scaling behavior perhaps takes place only in a very limited ξ -region [8].

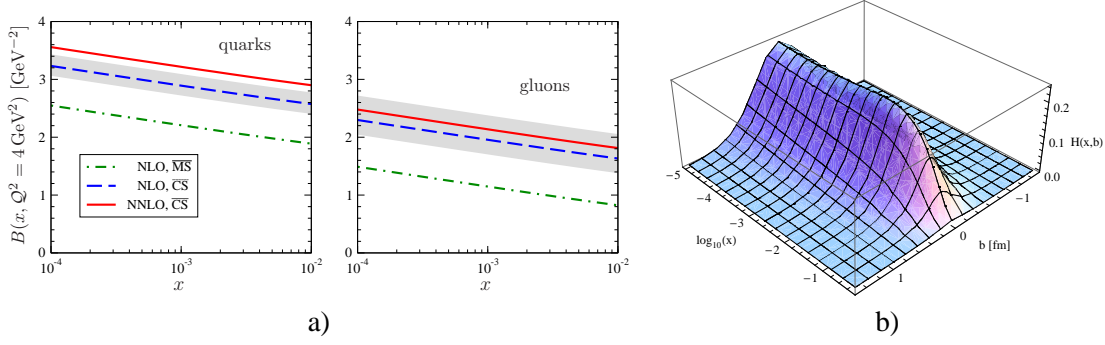


Fig. 4: a) Resulting GPD slope $B = \langle \mathbf{b}^2 \rangle / 4$ at the input scale $Q^2 = 4 \text{ GeV}^2$ and b) 3D picture of gluon GPD (23).

introduction, about the correlation of transversal and longitudinal degrees of freedom: partons with smaller momentum fractions are more decentralized. Intuitively, this small x partons might be somehow associated with the meson cloud that surrounds the proton center.

6 Summary

GPDs encode a unified description of the proton structure and they are experimentally accessible via the hard leptonproduction of photon or mesons. We have shown that the representation of Compton form factors as Mellin-Barnes integrals offers a useful tool in analyzing DVCS: the inclusion of evolution is simple, numerical treatment is stable and fast. Although the motivation for this representation originated from manifest conformal symmetry at LO, we have shown here that this Mellin-Barnes integral representation can be used within the standard $\overline{\text{MS}}$ scheme beyond LO. Such a representation can be straightforwardly obtained from the momentum fraction representation and, therefore, also other GPD related processes, e.g., the hard electroproduction of mesons, can be given in terms of Mellin-Barnes integrals. This opens a new road for the ‘global’ analysis of experimental data within the perturbative GPD formalism to NLO accuracy. Furthermore, the use of conformal symmetry enables elegant approach to higher-order radiative corrections to the DVCS amplitude. We have shown that although NLO corrections can be sizable, and are strongly dependent on the gluonic input, the NNLO corrections are small to moderate, supporting perturbative framework of DVCS. The observed change in the scale dependence is not so conclusive: similarly as in DIS we encounter large NNLO effects for $\xi < 10^{-3}$, which signal a breakdown of naive perturbation series expansion of the evolution operator. Nevertheless, this breakdown is universal and if we precisely define the treatment of this operator, perturbative QCD can be employed as a tool for analyzing data even in the small ξ region. We expect that within increasing accuracy in the perturbative approximation the GPD formalism improves.

Finally, fits to available DVCS and DIS data in collider kinematics work well in the collinear factorization approach beyond LO and give access to transversal distribution of partons. The lesson learned from the failure of LO fits can be extended to (oversimplified) GPD models used for phenomenology in fixed target kinematics. They do not possess a flexible skewness dependence parameterization and so the normalization of the amplitude for fixed t is mostly determined. Ironically, this non-flexibility originates from the implementation of PDF and form

factor constraints in the most convenient manner. This can be repaired in the Mellin-Barnes representation by a model dependent resummation of $SO(3)$ partial waves or in the momentum fraction representation by a more flexible double distribution ansatz, in which also the correlation of t - and skewness dependence is improved [17].

Additionally, we have observed that the off-shell Regge-exchange amplitudes [6], having the generic s -dependence of high-energy on-shell amplitudes, are ruled out. Repairing this failure yields the well-known dilemma of Regge-phenomenology. Namely, when extended to off-shell processes it fails to describe high energy data and must be improved, thereby losing its predictive power [38]. This loss of predictive power appears also in description of deeply exclusive leptonproduction data in the valence quark region within Regge inspired *models*, often outside of the accepted validity region $\{25 \text{ GeV}^2 \lesssim W^2, -t \lesssim 1 \text{ GeV}^2\}$ in classical Regge phenomenology, see e.g. [39]. Certainly, these approaches offer an easy and economical possibility to fit data and to interpret them in terms of mesonic exchanges and numerous couplings (unknown form factors). In our opinion the GPD formalism offers a new perspective for our QCD understanding, including a handle on the dynamical sources of Regge behavior. In this formalism one extracts information about non-perturbative quantities from experimental observables and interprets it in terms of partonic degrees of freedom. We consider Regge-inspired interpretations of data [40] as valuable tool for building realistic GPD models. This gives one handle more on the challenging task to understand hadron physics from QCD dynamics. Non-perturbative GPD aspects, in particular Regge behavior, might be studied within (partial) resummation of t -channel ladders (in the language of light-cone wave functions of higher partonic Fock states), e.g., Ref. [35,41], lattice simulations, and model building. This might lead to clues to improved understanding of hadron physics in terms of the underlying theory.

Acknowledgements

For illuminating discussions on Regge, BFKL, and collinear factorization approaches and their interplay as well as on GPD modelling we like to thank S. Brodsky, M. Diehl, B. Ermolaev, V. Fadin, D. Ivanov, L.L. Jenkovszky, P. Kroll, M. Polyakov, and A. Radyushkin. In particular, we are grateful to A. Szczepaniak for discussions on the work presented in Ref. [6]. D.M. is indebted to A. Miller, A.V. Efremov and O. Teryaev for invitation and support, allowing him to participate on *The 6th Circum-Pan-Pacific Symposium on High Energy Spin Physics* and the *XII Workshop on High Energy Spin Physics*, respectively. K. P-K. would like to thank the organizers of the *12th International Conference on Elastic and Diffractive Scattering*, DESY Hamburg, for invitation and support.

References

- [1] D. Müller, D. Robaschik, B. Geyer, F.-M. Dittes, and J. Hořejši, Fortschr. Phys. **42**, 101 (1994). hep-ph/9812448.
- [2] A. Radyushkin, Phys. Lett. **B380**, 417 (1996). hep-ph/9604317.
- [3] X.-D. Ji, Phys. Rev. Lett. **78**, 610 (1997). hep-ph/9603249.
- [4] A. V. Radyushkin, Phys. Rev. **D56**, 5524 (1997). hep-ph/9704207;
X.-D. Ji and J. Osborne, Phys. Rev. **D58**, 094018 (1998). hep-ph/9801260;
J. C. Collins and A. Freund, Phys. Rev. **D59**, 074009 (1999). hep-ph/9801262.

- [5] M. Diehl, Phys. Rept. **388**, 41 (2003). hep-ph/0307382;
A. V. Belitsky and A. V. Radyushkin, Phys. Rept. **418**, 1 (2005). hep-ph/0504030.
- [6] A. P. Szczepaniak, J. T. Londergan, and F. J. Llanes-Estrada (2007). 0707.1239 [hep-ph].
- [7] D. Müller and A. Schäfer, Nucl. Phys. **B739**, 1 (2006). hep-ph/0509204.
- [8] K. Kumerički, D. Müller, and K. Passek-Kumerički (2007). hep-ph/0703179.
- [9] D. Müller, Phys. Lett. **B634**, 227 (2006). hep-ph/0510109.
- [10] K. Kumerički, D. Müller, K. Passek-Kumerički, and A. Schäfer, Phys. Lett. **B648**, 186 (2007). hep-ph/0605237.
- [11] X.-D. Ji and J. Osborne, Phys. Rev. **D57**, 1337 (1998). hep-ph/9707254;
A. V. Belitsky and D. Müller, Phys. Lett. **B417**, 129 (1998). hep-ph/9709379;
L. Mankiewicz, G. Piller, E. Stein, M. Vanttinen, and T. Weigl, Phys. Lett. **B425**, 186 (1998). hep-ph/9712251.
- [12] D. Y. Ivanov, L. Szymanowski, and G. Krasnikov, JETP Lett. **80**, 226 (2004). hep-ph/0407207.
- [13] I. Gelfand and G. Shilov, *Generalized Functions*, Vol. I. Academic Press, New York, 1964.
- [14] A. Belitsky, A. Kirchner, D. Müller, and A. Schäfer, Phys. Lett. **B510**, 117 (2001). hep-ph/0103343.
- [15] O. V. Teryaev, Phys. Lett. **B510**, 125 (2001). hep-ph/0102303.
- [16] A. Radyushkin, Phys. Rev. **D56**, 5524 (1997). hep-ph/9704207;
A. V. Radyushkin (2000). hep-ph/0101225;
K. Goeke, M. Polyakov, and M. Vanderhaeghen, Prog. Part. Nucl. Phys. **47**, 401 (2001). hep-ph/0106012.
- [17] D. Hwang and D. Müller (2007). 0710.1567 [hep-ph].
- [18] D. Müller, Phys. Rev. **D49**, 2525 (1994);
A. V. Belitsky and D. Müller, Nucl. Phys. **B527**, 207 (1998). hep-ph/9802411;
A. V. Belitsky and D. Müller, Nucl. Phys. **B537**, 397 (1999). hep-ph/9804379.
- [19] A. Belitsky and A. Schäfer, Nucl. Phys. **B527**, 235 (1998);
B. Melić, B. Nžić, and K. Passek, Phys. Rev. **D65**, 053020 (2002). hep-ph/0107295.
- [20] D. Müller, Phys. Rev. **D58**, 054005 (1998). hep-ph/9704406;
D. Müller, Phys. Rev. **D59**, 116003 (1999). hep-ph/9812490;
B. Melić, D. Müller, and K. Passek-Kumerički, Phys. Rev. **D68**, 014013 (2003). hep-ph/0212346.
- [21] E. B. Zijlstra and W. L. van Neerven, Nucl. Phys. **B383**, 525 (1992);
A. Vogt, S. Moch, and J. A. M. Vermaseren, Nucl. Phys. **B691**, 129 (2004). hep-ph/0404111.
- [22] LHPC Collaboration, P. Hagler *et al.* (2007). arXiv:0705.4295 [hep-lat].
- [23] M. Polyakov and A. Shuvaev (2002). hep-ph/0207153.
- [24] M. Diehl and W. Kugler (2007). 0708.1121 [hep-ph].
- [25] D. Y. Ivanov, *Private communication* (unpublished). 2007.
- [26] C. Adloff *et al.*, Phys. Lett. **B517**, 47 (2001). hep-ex/0107005.
- [27] A. Aktas *et al.*, Eur. Phys. J. **C44**, 1 (2005). hep-ex/0505061.
- [28] S. Chekanov *et al.*, Phys. Lett. **B573**, 46 (2003). hep-ex/0305028.
- [29] S. Aid *et al.*, Nucl. Phys. **B470**, 3 (1996).
- [30] K. Kumerički, D. Müller, and K. Passek-Kumerički, <http://conferences.jlab.org/exclusive/talks/DMueller.pdf> (unpublished). 2007.
- [31] V. Guzey and T. Teckentrup, Phys. Rev. **D74**, 054027 (2006). hep-ph/0607099.
- [32] CLAS Collaboration, L. Morand *et al.*, Eur. Phys. J. **A24**, 445 (2005). hep-ex/0504057.
- [33] Jefferson Lab Hall A Collaboration, C. M. Camacho *et al.*, Phys. Rev. Lett. **97**, 262002 (2006). nucl-ex/0607029.

- [34] HERMES Collaboration, A. Airapetian *et al.* (2007). 0707.0222 [hep-ex].
- [35] I. Balitsky and E. Kuchina, Phys. Rev. **D 62**, 074004 (2000). hep-ph/0002195.
- [36] M. Burkardt, Phys. Rev. **D62**, 071503 (2000). hep-ph/0005108;
M. Burkardt, Int. J. Mod. Phys. **A18**, 173 (2003). hep-ph/0207047.
- [37] M. Strikman and C. Weiss, Phys. Rev. **D69**, 054012 (2004). hep-ph/0308191.
- [38] A. Donnachie and P. V. Landshoff, Phys. Lett. **B437**, 408 (1998). hep-ph/9806344;
M. Capua, S. Fazio, R. Fiore, L. Jenkovszky, and F. Paccanoni, Phys.Rev. **D75**, 116005 (2007).
hep-ph/0605319.
- [39] F. Cano and J. M. Laget, Phys. Lett. **B551**, 317 (2003). hep-ph/0209362.
- [40] J. M. Laget (2007). 0708.1250 [hep-ph].
- [41] B. I. Ermolaev, M. Greco, and S. I. Troyan, Nucl. Phys. **B594**, 71 (2001). hep-ph/0009037.